A METHOD OF REPRESENTING THE HORIZONTAL PRESSURE FORCE WITHOUT REDUCTION OF STATION PRESSURES TO SEA LEVEL[1]

Wayne E. Sangster

The University of Chicago

(Original manuscript received 13 July 1959; revised manuscript received 1 October 1959)

ABSTRACT

A coordinate system is presented in which the lowest coordinate surface represents the topography of the earth. Higher coordinate surfaces reflect this topography in diminishing degrees and become isobaric at and above the 500-mb level. A method of representing the field of the horizontal pressure force in the nonisobaric coordinate surfaces, using geostrophic stream and potential functions, is described. Geostrophic winds computed from these functions are compared with those obtained from the customary sea-level charts and with observed winds.

1. Introduction

Charts depicting the atmospheric conditions in isobaric surfaces are now generally used in conventional as well as numerical forecasting. These charts have the advantage, first enunciated by Bjerknes and Sandström (1910), that the horizontal pressure force may be represented by a single scalar field, namely that of the geopotential of an isobaric surface. Isobaric charts obviously cannot be used for depicting conditions at the earth's surface, and the problem of computing and representing the field of the horizontal pressure force becomes more complicated at and near the earth's surface. The procedure of reducing barometer readings of land stations to some standard reference level, such as sea level or 1000 mb, may give rise to intolerable errors in the field representing the horizontal pressure force.

The research described in this article is primarily concerned with the problem of computing and representing the field of the horizontal pressure force in nonisobaric surfaces. Also, a coordinate system is presented in which the earth's surface (or some smoothed version of it) is one of the coordinate surfaces. With increasing elevation the coordinate surfaces approach isobaricity, and above some suitably chosen level all coordinate surfaces are isobaric.

2. The coordinate system

Phillips (1957) has introduced a coordinate system in which pressure (p) is replaced as the vertical coordinate by the independent variable $\sigma \equiv p/\pi$, where π is the pressure at the ground. This system has the advantage that the earth's surface is a coordinate surface—namely that defined by $\sigma = 1$. However, it has the disadvantage that only the coordinate surface $\sigma = 0$ is isobaric, thus losing the benefits to be derived from the use of isobaric surfaces in the analysis and forecasting of conditions some distance above the earth's surface.

Definition of the new independent variables. The advantages of the σ-system and those of the p-system may be combined by introducing the independent variables P and P', defined by

$$(p \geq p_5) \qquad P \equiv 5\left(\frac{p - p_5}{p_{10} - p_5} + 1\right), \tag{1a}$$

$$(p \leq p_5) \qquad P' \equiv \frac{5p}{p_5} \tag{1b}$$

where p_{10} is the pressure at the ground and $p_5 \equiv 500$ mb. We assume that p_{10} is everywhere greater than p_5. P is to be used when $p \geq p_5$, while P' is to be used when $p \leq p_5$. It will be seen that P ranges monotonically from 10 at the ground to 5 at 500 mb, and P' ranges monotonically from 5 at 500 mb to zero at the top of the atmosphere. This system has the advantage that all coordinate surfaces at and above the 500-mb level are isobaric surfaces. The choice of 500 mb as the level of transition from isobaric to nonisobaric coordinate surfaces is arbitrary, and other levels may be chosen depending upon the height of the terrain.

General relations. In the following, partial differentiation in the P, P'-system will carry no subscript, while differentiation in the p-system will carry the subscript p. The relations between partial differentiations in the two coordinate systems are

$$(p \geq p_5) \qquad \frac{\partial}{\partial t} = \left(\frac{\partial}{\partial t}\right)_p + \frac{P - 5}{p_{10} - p_5}\frac{\partial p_{10}}{\partial t}\frac{\partial}{\partial P}, \tag{2a}$$

$$(p \leq p_5) \qquad \frac{\partial}{\partial t} = \left(\frac{\partial}{\partial t}\right)_p \tag{2b}$$

[1] The research reported in this article has been sponsored by the Geophysics Research Directorate of the Air Force Cambridge Research Center, Air Research and Development Command, under Contract No. AF19(604)-2179.

and

$$(p \geq p_5) \qquad \nabla = \nabla_p + \frac{P-5}{p_{10}-p_5}\nabla p_{10}\frac{\partial}{\partial P}, \tag{3a}$$

$$(p \leq p_5) \qquad \nabla = \nabla_p. \tag{3b}$$

The operator d/dt may be written as

$$(p \geq p_5) \qquad \frac{d}{dt} \equiv \frac{\partial}{\partial t} + V\cdot\nabla + \Omega\frac{\partial}{\partial P}, \tag{4a}$$

$$(p \leq p_5) \qquad \frac{d}{dt} \equiv \frac{\partial}{\partial t} + V\cdot\nabla + \Omega'\frac{\partial}{\partial P'} \tag{4b}$$

where V is the horizontal component of the wind, $\Omega \equiv dP/dt$, and $\Omega' \equiv dP'/dt$.

From (1), (2), (3), and (4), we obtain the following for the relation between Ω and Ω' at 500 mb ($P = P' = 5$):

$$\Omega(5) = \frac{p_5}{p_{10}-p_5}\Omega'(5).$$

As kinematic boundary conditions, we have $\Omega = 0$ at $P = 10$, and $\Omega' = 0$ at $P' = 0$.

The altimeter correction system. Since the altimeter correction system of Bellamy (1945) will be used later, some general equations referring to that system will be presented here. The hydrostatic equation may be written as

$$\frac{\partial D}{\partial Z_p} = S^* \tag{5}$$

or

$$\frac{\partial D}{\partial Z} = \frac{S^*}{1+S^*}. \tag{6}$$

Here, $S^* \equiv (T^* - T_p)/T_p$ and $D \equiv Z - Z_p$, where D is the altimeter correction, S^* is the specific virtual temperature anomaly, T^* is the virtual temperature, T_p is the temperature in the standard atmosphere corresponding to the pressure at the point under consideration, Z is the height above mean sea level, and Z_p is the pressure altitude.

The hydrostatic equation for the standard atmosphere may be written as

$$\frac{dZ_p}{dp} = -\frac{\alpha_p}{g_p} \tag{7}$$

where α_p is the specific volume of the standard atmosphere and g_p is the standard acceleration of gravity.

We may write

$$\nabla = \nabla_p + \nabla Z_p\frac{\partial}{\partial Z_p} \tag{8}$$

which may be used as an alternative to (3a).

The horizontal pressure force. By applying (3a) to Z, we find that the slope of an isobaric surface intersecting a coordinate surface is given by

$$(p \geq p_5) \qquad \nabla_p Z = \nabla Z - \frac{P-5}{p_{10}-p_5}\frac{\partial Z}{\partial P}\nabla p_{10}. \tag{9}$$

Since the slope of the earth's surface may be an order of magnitude or more greater than the slope of an isobaric surface, the slope of an isobaric surface computed from (9) may come out as the difference between two large terms, thus making the accuracy of the computations extremely doubtful.

Schemes using pressure parameters which are departures from mean or standard atmosphere values have been proposed by Fujita and Brown (1957) and Harrison (1958) as a means of overcoming this difficulty. The parameters proposed by these authors are defined with Z as the vertical coordinate, and are, therefore, not convenient for use in a system where pressure is the vertical coordinate. On the other hand, the altimeter correction system of Bellamy has been found to be quite convenient for the purpose of computing the horizontal pressure force in isobaric as well as in nonisobaric surfaces.

By applying (8) to D, and by substituting from (5), we obtain

$$\nabla_p D = \nabla_p Z = \nabla D - S^*\nabla Z_p. \tag{10}$$

The advantage of (10) over (9) is that ∇Z_p is multiplied by S^*, a quantity normally ranging from -0.2 to $+0.1$, so that the accuracy of the computations is substantially increased.

The equations of horizontal motion in the P, P'-system may be obtained from the corresponding equations in the p-system with the aid of (4) and (10).

The equation of continuity. The equation of continuity in the P, P'-system may be written as

$$(p \geq p_5) \qquad \nabla\cdot V + \frac{\partial\Omega}{\partial P} + \frac{1}{p_{10}-p_5}\left(\frac{\partial p_{10}}{\partial t} + V\cdot\nabla p_{10}\right) = 0,$$

$$(p \leq p_5) \qquad \nabla\cdot V + \frac{\partial\Omega'}{\partial P'} = 0.$$

That this is so may be ascertained by transforming the equation of continuity with pressure as the vertical coordinate with the aid of the appropriate relations between the two coordinate systems.

The hydrostatic equation. Since pressure altitude rather than pressure is the independent variable in (5), this equation is not directly transformable into the P, P'-system. An equation which can be directly transformed may be obtained by introducing a quantity which we shall call the specific volume anomaly (α'), defined by $\alpha' \equiv \alpha - \alpha_p$, where α is the specific volume. It follows from (7) and the hydrostatic equation in the p-system that

$$(p \geq p_5) \qquad \frac{\partial D}{\partial P} = -\frac{(p_{10}-p_5)}{5}\frac{\alpha'}{g},$$

$$(p \leq p_5) \qquad \frac{\partial D}{\partial P'} = -\frac{p_5}{5}\frac{\alpha'}{g}$$

where g is the acceleration of gravity, and the difference between g and g_p has been neglected.

The first law of thermodynamics. With α' as a variable, this law may be written as

$$(p \geq p_5) \quad \frac{\partial \alpha'}{\partial t} = - V \cdot \nabla \alpha' + \frac{p_{10} - p_5}{5} (\Lambda_d - \Lambda)\Omega + \tfrac{1}{5}\Lambda_d (P - 5) \times \left(\frac{\partial p_{10}}{\partial t} + V \cdot \nabla p_{10} \right) + \frac{R}{pc_p} \dot{W},$$

$$(p \leq p_5) \quad \frac{\partial \alpha'}{\partial t} = - V \cdot \nabla \alpha' + \frac{p_5}{5} (\Lambda_d - \Lambda)\Omega' + \frac{R}{pc_p} \dot{W}$$

where Λ_d is the dry adiabatic rate of change of α' with respect to pressure, $\Lambda \equiv \partial \alpha' / \partial p$, c_p is the specific heat of air at constant pressure, R is the gas constant of air, and $\dot{W}$ is the nonadiabatic rate of heating of a unit mass. The first of these equations states that the local rate of change of α' is composed of four parts: (1) the change due to advection of α' in a coordinate surface by the horizontal wind; (2) the combined adiabatic-vertical advection change due to motion with respect to coordinate surfaces; (3) the adiabatic change arising from the nonisobaricity of the coordinate surfaces; and (4) the change due to nonadiabatic heating or cooling.

The reference surface. Since the topography of the earth's surface contains features with dimensions which are much smaller than those of synoptic-scale weather systems, the coordinate surface $P = 10$ will here be defined as some highly smoothed representation of the actual earth's surface. This procedure will necessitate reducing station pressures to this reference surface, but the depth of the layer through which this reduction is made will generally be much less than the depth of the layer through which pressures are reduced to sea level. Furthermore, the reference surface may be defined so that the reduction will be upward for many of the stations. The introduction of the smoothed reference surface gives rise to a certain degree of fictitiousness for P-levels near the ground, but this would seem to be unavoidable.

3. Representation of the horizontal pressure force using geostrophic stream and potential functions

The geostrophic stream and potential functions. Equation (10) may be used to compute the horizontal pressure force in a nonisobaric surface if charts of S^*, D, and Z_p for that surface are available. The presence of three variables might be of little consequence to a machine in making a forecast, but, since both the current and prognostic charts must be interpreted by the forecaster, it is desirable to represent the horizontal pressure force in a less complicated manner. Since the horizontal pressure force is a two-dimensional vector, we may expect, in general, that a minimum of two scalar fields will be needed for its representation. In special cases, such as for isobaric or isentropic surfaces, or for constant S^*, one scalar field suffices.

Any two-dimensional vector field may be decomposed into a nondivergent part, representable by a stream function, and an irrotational part, representable by a potential function. Denoting the geostrophic stream function by H and the geostrophic potential function by G, we may write

$$\nabla_p Z \times \boldsymbol{k} = m(\nabla_{(m)} H \times \boldsymbol{k} + \nabla_{(m)} G). \tag{11}$$

Here, m is the scale factor of the chart, and

$$\nabla_{(m)} \equiv \boldsymbol{i} \frac{\partial}{\partial x} + \boldsymbol{j} \frac{\partial}{\partial y}$$

where x and y are the independent variables of a Cartesian coordinate system on a conformal map projection. The problem is to compute $G(x, y)$ and $H(x, y)$ so as to satisfy (11).

Computation of H and G. In terms of the Cartesian coordinate system, (10) becomes

$$\nabla_p Z = m(\nabla_{(m)} D - S^* \nabla_{(m)} Z_p). \tag{12}$$

From (11) and (12), we obtain

$$\nabla_{(m)} B \times \boldsymbol{k} - \nabla_{(m)} G = S^* \nabla_{(m)} Z_p \times \boldsymbol{k} \tag{13}$$

where $B \equiv D - H$. By taking the divergence and the vertical component of the curl of (13), we obtain, respectively,

$$\nabla_{(m)}{}^2 G = J_{(m)}(Z_p, S^*) \tag{14}$$

and

$$\nabla_{(m)}{}^2 B = S^* \nabla_{(m)}{}^2 Z_p + \nabla_{(m)} S^* \cdot \nabla_{(m)} Z_p \tag{15}$$

where $J_{(m)}(Z_p, S^*)$ is the Jacobian determinant of Z_p and S^* with respect to x and y. If boundary conditions are specified, (14) and (15) may be solved for G and B. From (13), we find that the conditions applicable at the boundary are

$$\frac{\partial B}{\partial n} + \frac{\partial G}{\partial s} = S^* \frac{\partial Z_p}{\partial n} \tag{16}$$

and

$$\frac{\partial B}{\partial s} - \frac{\partial G}{\partial n} = S^* \frac{\partial Z_p}{\partial s} \tag{17}$$

where s and n measure length along and normal to the boundary, respectively. For convenience, we shall introduce the convention that n will be positive along the exterior normal and the positive progression along the border will be counter-clockwise.

In solving (14) and (15), we may, as boundary conditions, specify either the values of B and G

(Dirichlet conditions) or the normal gradients of B and G (Neumann conditions). Since there is evidence that the relaxation procedure with the Neumann conditions is slow to converge, it is desirable to use the Dirichlet conditions for both equations. This may be done in either of two ways. We may prescribe B arbitrarily on the boundary and solve (15). Knowing B as a function of x and y, we may compute $\partial B/\partial n$ along the boundary. Next, the boundary values of $\partial G/\partial s$ are obtained from (16). Stepwise integration of $\partial G/\partial s$ from point-to-point starting at any boundary point with an arbitrary value will give G at all boundary points. Equation (14) may then be solved for $G(x, y)$. The alternative method is to prescribe G arbitrarily on the boundary and subsequently to compute boundary values of B which are consistent with (17).

The question arises as to whether this choice of boundary values insures that (13) is satisfied everywhere. Let us assume that the computed $G(x, y)$ is not consistent with the computed $B(x, y)$, so that (13) is not satisfied. Let $G(x, y) = G_1(x, y) + G_2(x, y)$, where $G_1(x, y)$ is known to be consistent with the computed $B(x, y)$. Then $\nabla_{(m)}{}^2G = \nabla_{(m)}{}^2G_1$, and $\nabla_{(m)}{}^2G_2 = 0$. G and B satisfy either (16) or (17), depending upon the method chosen for specifying the boundary conditions, and it follows that either $\partial G_2/\partial s = 0$ or $\partial G_2/\partial n = 0$ on the boundary, since G_1 also satisfies (16) and (17). Therefore, $G_2(x, y)$ is a constant. The constant is irrelevant, so our choice of boundary conditions is appropriate.

The finite-difference grid. Equations (14) and (15) may be solved by using finite differences and the well known relaxation methods. If we were to use the same lattice to solve both (14) and (15), a difficulty would arise in the specification of boundary conditions, since a centered normal derivative could not be computed at the boundary. This difficulty can be overcome simply by using two lattices as shown in fig. 1. The lattice of squares is used in solving the equation for which the unknown is specified arbitrarily on the boundary, and the lattice of circles is used in solving the other equation. With this arrangement, a normal derivative near the boundary of the lattice of squares is centered at the same point as a tangential derivative at the boundary of the lattice of circles, so uncentered finite differences do not arise.

By using the customary symbol $\oint$ for integrals along a closed curve, it is of interest to note that, though

$$\oint \frac{\partial B}{\partial s}\,ds \quad \text{or} \quad \oint \frac{\partial G}{\partial s}\,ds$$

vanishes, the substitution of finite differences will usually leave a residual. Some adjustment of the boundary values is necessary to remove this residual.

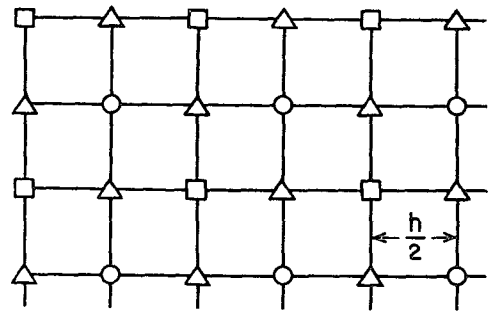

FIG. 1. A portion of the grid used in computing the geostrophic stream and potential functions. The lattice of squares is used in solving one of equations (14) and (15), and the lattice of circles is used in solving the other. The triangles are used to compute first derivatives.

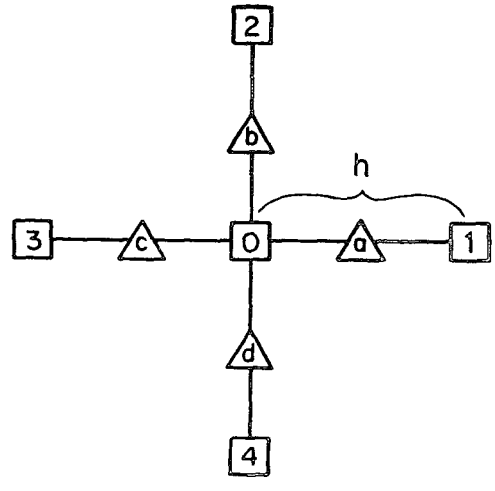

FIG. 2. Finite-difference grid.

The appropriate finite-difference approximations are readily obtained by using a finite-difference grid as shown in fig. 2. The squares are used to compute second derivatives and the triangles are used to compute first derivatives, so that the same mesh size (h) is used for both types of derivatives.

Representation of the horizontal pressure force over the oceans. At sea level over the oceans, (10) becomes

$$(\nabla_p Z)_{10} = (1 + S_{10}{}^*)\nabla D_{10}. \tag{18}$$

An alternative equation for computing the horizontal pressure force over the oceans is obtained by defining a new variable D_s such that

$$D_s \equiv D - S^*(Z_p - Z_{ps}) \tag{19}$$

where Z_{ps} is the pressure altitude which would exist at the P-level under consideration if D_{10} were everywhere zero. Thus, Z_{ps} is constant for any given P-level and $Z_{p10} - Z_{ps10} = -D_{10}$. By substituting from (19) into (10), we obtain

$$\nabla_p Z = \nabla D_s + (Z_p - Z_{ps})\nabla S^*.$$

At sea level, this becomes

$$(\nabla_p Z)_{10} = \nabla D_{s10} - D_{10}\nabla S_{10}^*. \quad (20)$$

It should be noted that D_{10} in (18) corresponds to the sea-level pressure, whereas D_{s10} in (20) corresponds to the 1000-mb height (actually, it is the 1013.25-mb D-value). When the horizontal pressure force is computed from sea-level isobars, the density is usually assumed to be a constant. This is equivalent to using a constant S_{10}^* in (18). The second term on the right of (20) corresponds to the error introduced by reducing sea-level pressures to 1000-mb heights.

It would seem unnecessary to compute geostrophic stream and potential functions over the oceans, since D or D_s is roughly equivalent to the stream function, and the potential function field would be rather flat.

Selection of boundary conditions. As mentioned previously, we may specify arbitrarily either G or B on the outer boundary. Values of B or G for the inner boundary are then determined from (16) or (17). A two-dimensional vector field which is both nondivergent and irrotational may be represented by either a stream function or a potential function alone, and the specification of boundary conditions determines the manner in which the nondivergent, irrotational part of the horizontal pressure force field is divided between the stream and potential functions.

If we are to use charts of the stream function in conjunction with charts of D or D_s for the oceanic areas it is desirable to choose boundary values of B such that $H = D$ or $H = D_s$ at those boundary points which are at sea level. This requires that at the sea-level boundary points either $B=0$ or $B=S^*(Z_p-Z_{ps})$, depending upon whether D or D_s is used.

This leaves the problem of specifying boundary values at points not at sea level. It is desirable to represent as much as possible of the field of the horizontal pressure force by the stream function. Therefore, we shall choose boundary conditions so that we minimize

$$\int\int (\nabla_{(m)}G)^2 dxdy$$

where the integration extends over the entire area under consideration. From (13), we see that

$$\int\int (\nabla_{(m)}G)^2 dxdy = \int\int (\nabla_{(m)}B - S^*\nabla_{(m)}Z_p)^2 dxdy. \quad (21)$$

By equating the variation of the right-hand side of (21) to zero, we have

$$\int\int [(\nabla_{(m)}B - S^*\nabla_{(m)}Z_p)\cdot\nabla_{(m)}\delta B]dxdy = 0$$

which may be transformed into

$$\int\int \delta B(\nabla_{(m)}{}^2 B - S^*\nabla_{(m)}{}^2 Z_p - \nabla_{(m)}S^*\cdot\nabla_{(m)}Z_p)dxdy - \oint \delta B\left(\frac{\partial B}{\partial n} - S^*\frac{\partial Z_p}{\partial n}\right)ds = 0$$

where the line integral is taken along the boundary of the area over which the double integral extends. Since δB is zero at boundary points where B has been prescribed and arbitrary at all other boundary points and at all interior points, this requires that (a) equation (15) be satisfied at all interior points and (b) $\partial B/\partial n = S^*\partial Z_p/\partial n$ at all boundary points where B has not been prescribed. Requirement (a) is already met, and (b) completes the specification of boundary conditions, which are mixed (Dirichlet-Neumann) conditions.

For some purposes, it may be desirable to specify boundary values of G arbitrarily and let the boundary values of B fall where they may. From (16), requirement (b) above gives us $G(s)$ = constant as the appropriate boundary conditions for minimizing $\int\int (\nabla_{(m)}G)^2 dxdy$.

The geostrophic wind in terms of H and G. From (11), we see that the geostrophic-wind equation with H and G as the variables is

$$\boldsymbol{V}_g = -\frac{gm}{f}[\nabla_{(m)}H \times \boldsymbol{k} + \nabla_{(m)}G]$$

where $\boldsymbol{V}_g$ is the geostrophic wind and f is the Coriolis parameter. It will be seen that the geostrophic wind is computed as the sum of two components. One of these is *parallel* to the isopleths of H, while the other is *perpendicular* to the isopleths of G. The magnitude of each component is inversely proportional to the spacing of the corresponding isopleths. H and G are expressed in units of height, and the geostrophic wind scales used for isobaric analysis may be used in connection with the H- and G-charts.

Discontinuities in the fields of H and G. Since fronts are usually represented as first-order discontinuities in the sea-level pressure field, the question arises as to what types of discontinuities are present in the H- and G-fields. In the following, frontal surfaces will be treated as zero-order discontinuities in the virtual temperature field.

It is convenient to choose the x-axis along the projection onto a level surface of the line of intersection between the frontal surface and a coordinate surface, such that the positive y-axis lies in the cold air. Conditions in the warm air will be denoted by the subscript w, while the subscript c refers to the cold air.

The slope of a frontal surface in the yZ_p-plane is

given by

$$\frac{\delta Z_p}{\delta y} = \frac{\left(\frac{\partial D_c}{\partial y}\right)_p - \left(\frac{\partial D_w}{\partial y}\right)_p}{S_w^* - S_c^*}.$$

By writing the appropriate component equation obtained from (11) for conditions in the warm air and in the cold air and making use of the facts that $\delta Z_p/\delta y > 0$ for all fronts and that $\partial G_c/\partial x = \partial G_w/\partial x$, we find that $\partial H_c/\partial y - \partial H_w/\partial y > 0$. Thus, the kink in the isopleths of H always points from low to high values, a circumstance which might have been suspected. Not so obvious, however, is the situation concerning the isopleths of G. Since $\partial B_c/\partial x = \partial B_w/\partial x$, it follows from (13) that $\partial G_c/\partial y - \partial G_w/\partial y > 0$ if $\partial Z_{pc}/\partial x = \partial Z_{pw}/\partial x = \partial Z_p/\partial x < 0$, and $\partial G_c/\partial y - \partial G_w/\partial y < 0$ if $\partial Z_p/\partial x > 0$. The kink in the isopleths of G points toward higher values when $\partial Z_p/\partial x < 0$ and toward lower values when $\partial Z_p/\partial x > 0$. No discontinuity in the field of G is present when $\partial Z_p/\partial x = 0$.

4. A variable reference atmosphere

Equation (10) has the advantage over (9) that the vertical variation of D is much less than that of Z; hence, the magnitude of the second term on the right of (10) is much smaller than that of the second term on the right of (9). Equation (10) is still somewhat unsatisfactory, however, since the magnitude of the second term on the right depends upon how the standard atmosphere is defined. This suggests that an improvement upon (10) could be made so that the effect of sloping terrain upon the computations is minimized. The problem is the subject of this section.

Definition of the reference atmosphere. We may define a reference atmosphere whose properties may be varied at will in the following manner. Let the specific temperature anomaly of this reference atmosphere (S_r) be defined as a constant in the vertical, but variable with x and y. By integrating the hydrostatic equation (5) from some arbitrary base level ($\hat{Z}_v$) to Z_p, we have

$$D_r = S_r(Z_p - \hat{Z}_p) \tag{22}$$

where the D-value in the reference atmosphere (D_r) has been taken as zero at the base level $\hat{Z}_v$. $\hat{Z}_p$ will be defined as a constant.

Let Z_r be height in the reference atmosphere. Then, using (22), we have

$$Z_r = Z_p + D_r = Z_p + S_r(Z_p - \hat{Z}_p). \tag{23}$$

By defining the altimeter correction with respect to the new reference atmosphere by $D' \equiv Z - Z_r$, we find from (23) that

$$D' = D - S_r(Z_p - \hat{Z}_p). \tag{24}$$

D' is the new pressure variable, replacing D.

Selection of S_r and $\hat{Z}_p$. Ideally, S_r and $\hat{Z}_p$ should be specified so as to minimize the influence of topography upon the computations. By substituting from (24) into (12), we obtain

$$\nabla_p Z = m[\nabla_{(m)} D' - (S^* - S_r)\nabla_{(m)} Z_p + (Z_p - \hat{Z}_p)\nabla_{(m)} S_r].$$

The condition used to specify S_r is that

$$\int\int \{[(S^* - S_r)\nabla_{(m)} Z_p]^2 + [(Z_p - \hat{Z}_p)\nabla_{(m)} S_r]^2\} dxdy \tag{25}$$

is to be minimized. Equating the variation of (25) to zero, we have

$$\int\int [\delta S_r (S^* - S_r)(\nabla_{(m)} Z_p)^2 - (Z_p - \hat{Z}_p)^2 \nabla_{(m)} S_r \cdot \nabla_{(m)} \delta S_r] dxdy = 0$$

which may be rewritten as

$$\int\int \delta S_r [(S^* - S_r)(\nabla_{(m)} Z_p)^2 + (Z_p - \hat{Z}_p)^2 \nabla_{(m)}{}^2 S_r + 2(Z_p - \hat{Z}_p)\nabla_{(m)} Z_p \cdot \nabla_{(m)} S_r] dxdy - \oint \delta S_r (Z_p - \hat{Z}_p)^2 \frac{\partial S_r}{\partial n} ds = 0.$$

Since δS_r is arbitrary, this requires that at all interior points

$$\nabla_{(m)}{}^2 S_r + \frac{2\nabla_{(m)} Z_p \cdot \nabla_{(m)} S_r}{Z_p - \hat{Z}_p} + \frac{S^* - S_r}{(Z_p - \hat{Z}_p)^2} (\nabla_{(m)} Z_p)^2 = 0 \tag{26}$$

and on the boundary

$$\frac{\partial S_r}{\partial n} = 0. \tag{27}$$

In finite-difference form, with reference to fig. 2, (26) becomes

$$(1 + \gamma_x)S_{r1} + (1 + \gamma_y)S_{r2} + (1 - \gamma_x)S_{r3} + (1 - \gamma_y)S_{r4} - (4 + \gamma^2)S_{r0} + \gamma^2 S_0^* = 0 \tag{28}$$

where

$$\gamma_x \equiv \frac{Z_{pa} - Z_{pc}}{Z_{p0} - \hat{Z}_p},$$

$$\gamma_y \equiv \frac{Z_{pb} - Z_{pd}}{Z_{p0} - \hat{Z}_p},$$

and

$$\gamma^2 \equiv \gamma_x{}^2 + \gamma_y{}^2.$$

Equation (28) can be solved by relaxation methods, using boundary conditions given by (27). Collatz (1955) has shown that a sufficient condition for the convergence of the relaxation procedure is that the coefficients $1 \pm \gamma_x$ and $1 \pm \gamma_y$ all be positive quantities. The logical choice for $\hat{Z}_p$ is then a value which will just meet this condition.

In terms of D', (15) becomes

$$\nabla_{(m)}{}^2B' = (S^* - S_r)\nabla_{(m)}{}^2Z_p + \nabla_{(m)}Z_p \cdot \nabla_{(m)}(S^* - 2S_r) - (Z_p - \hat{Z}_p)\nabla_{(m)}{}^2S_r \quad (29)$$

where $B' \equiv D' - H$. Equation (14) is unaffected by the change of variable.

Since a great deal of computational work is involved in the method described above, a simpler method will be useful. As a first approximation, we may put $S_r = \hat{S}_r$, where $\hat{S}_r$ is a linear function of y only. This prevents $\nabla_{(m)}\hat{S}_r$ from becoming excessive, while at the same time the usual north-south temperature gradient can be allowed for. $\hat{S}_r(y)$ is chosen by attempting to minimize $|S^* - \hat{S}_r|$ in those areas where $\nabla_{(m)}Z_p$ is large.

5. Comparison between customary sea-level charts and charts of the geostrophic stream and potential functions

The purpose of this comparison is to ascertain whether charts of the geostrophic stream and potential functions for the lowest coordinate surface provide a better relation between the actual wind and the apparent geostrophic wind than do charts of pressure reduced to sea level. The difference between the two methods of representation will be large where strong temperature gradients exist in connection with elevated terrain. For this reason, the area covered in the comparison includes the Great Plains and the Rocky Mountains, and a rather extreme winter situation has been chosen so as to provide large temperature contrasts.

Sources of data. Temperatures, altimeter settings, 850-mb heights, and sea-level pressures from over 450 stations were used in the computation of the geostrophic stream and potential functions. Most of the D-values were computed from the altimeter settings reported in the airways observations. Since not all stations report altimeter settings, 850-mb heights reported in the surface observations and sea-level pressures were used as supplementary sources of information for computing D-values. The D-value at the ground was obtained by following a procedure which was essentially a reversal of the process used to compute the 850-mb height or sea-level pressure in the first place. Since sea-level pressure computations for stations more than 1000 ft above MSL involve an assumed lapse rate, a correction for moisture, and a plateau correction, no attempt was made to utilize sea-level pressures for such stations.

A high-speed electronic computer was used to compute D- and S^*-values from the teletype data. The D-values at the reference surface were obtained by integration of (6) between the ground and the reference surface, under the assumption that S^* is a constant within this layer. This is equivalent to assuming a lapse rate in this layer equal to that of the standard atmosphere. In keeping with the above assumption, S^* at the reference surface was assumed to be the same as that at the ground.

Some computational details. A variable reference atmosphere was used for all computations of the stream function. The specific temperature anomaly of this reference atmosphere was defined by using the simplified procedure described at the end of section 4. The constant $\hat{Z}_p$ was chosen to be zero in all cases.

Values of S^* and D at grid points were obtained from smoothed analyses. The values of G and B' at grid points were obtained by solving (14) and (29). Values of B' at the observation stations were obtained from the analyses of the B'-fields, and the values of the stream function at the observation stations were then computed. An alternative procedure is to read off the D'-values at grid points and to compute the H-values at grid points rather than at observation stations. This procedure would require a smoothing operation on the D'-field to adjust for inaccurate and unrepresentative observations. It was felt, however, that the smoothing operation should be performed on the H-field rather than on the D'-field, since the physical significance of the gradient of the stream function is more readily interpreted than is that of the D'-value.

In computing the values of H and G to be discussed in connection with fig. 4, the conditions at the boundary were specified so that $G = 0$ along the entire boundary. This minimizes the contribution of the potential function but does not allow the arbitrary specification of boundary values of B' at sea-level boundary points. The arbitrary constants in the B'-fields were chosen so that $H = D$ at a point approximately midway along the eastern boundary.

The mesh size of the finite-difference grid used in computing the stream and potential functions was chosen to be 131 km (at 45 deg lat), a value considered to be consistent with the station density of the observational network.

Construction of the reference surface. The reference surface used in the computations is shown in fig. 3. The data used to construct this surface consisted of terrain elevations averaged over overlapping areas of one degree latitude by one degree longitude. In some areas, a considerable amount of smoothing was necessary to eliminate small-scale features which could not be resolved by the finite-difference grid with a mesh size of 131 km.

The temperature field. The period chosen for the comparison was one during which a vast mass of arctic air moved southward over the Great Plains and became adjacent to a mass of tropical air. The thermal properties of the air masses involved are shown in the upper charts of fig. 4. In the early hours of 8 January, arctic air invaded Montana and part of North Dakota. During the following 48 hr, the arctic air moved

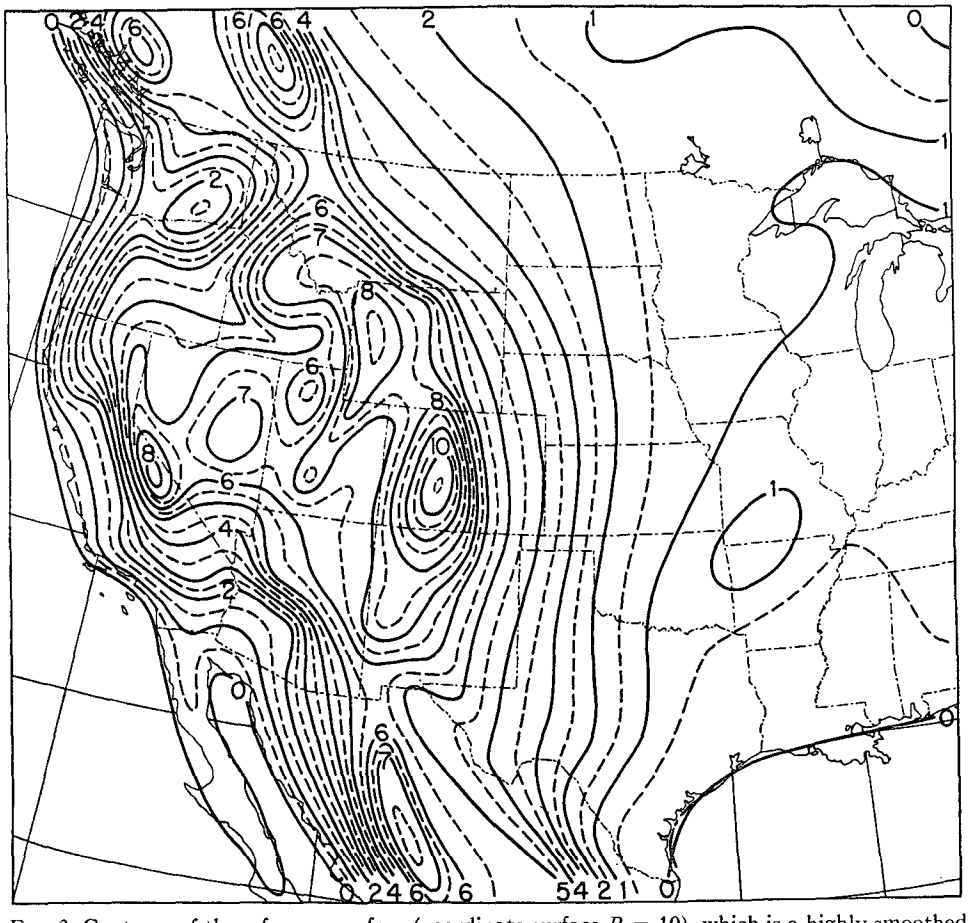

FIG. 3. Contours of the reference surface (coordinate surface $P = 10$), which is a highly smoothed representation of the earth's surface. Unit of height is 1000 ft.

rapidly southward and, together with tropical air from the Gulf of Mexico, created a band of strong temperature contrast from New Mexico toward the Appalachians. During this period, the cold air piled up against the eastern slope of the Rocky Mountains, leaving relatively warm air to the west. It will be seen that the situation chosen for comparison affords strong temperature contrasts in connection with a large variety of terrain features.

Referring back to equation (14), it will be seen that the potential function becomes important in regions where the angle between the gradients of the specific virtual temperature anomaly and the terrain approaches a right angle and the magnitudes of these gradients are large. Of particular interest for the later discussion is the large temperature gradient present on the afternoon of 9 January over the panhandles of Texas and Oklahoma. At 1830 GCT 9 January, the surface temperature at Amarillo, Texas was 68F, while about 100 mi to the north at Guymon, Oklahoma the temperature was 17F.

Charts of the stream and potential functions compared with sea-level charts. Isopleths of H and G are shown in the center charts of fig. 4, and sea-level isobars are shown in the lower charts. It will be seen that the charts for 0630 and 1830 GCT 8 January show a marked concentration of the H-isopleths along the Continental Divide in Montana and Canada. While this packing is not as extreme as on the sea-level charts, it still corresponds to a large geostrophic wind. A study of conditions at Lethbridge, Alberta (elevation 3018 ft), to the east of the Continental Divide, and at Kimberley, British Columbia (elevation 3016 ft), to the west of the Divide, is of interest. At 0630 GCT 8 January, the D-values at the ground at Lethbridge and Kimberley were +160 ft and −270 ft, respectively, and the corresponding temperatures were −10F and +22F. Since these two stations are at nearly the same elevation, the difference in the D-values is a measure of the horizontal pressure force in a level surface passing through the two stations.

The above conditions correspond to a geostrophic-wind component normal to the line connecting the two stations of about 90 kn. While the ground-level D-values at the two stations are real, the corresponding geostrophic wind is fictitious because of the presence of the intervening mountain range. Presumably, if one were to compute the horizontal pressure force along the actual earth's surface instead of along a fictitious, level surface, a lower value would result. The reference surface in this area is a poor representation of the actual earth's surface, and the stream func-

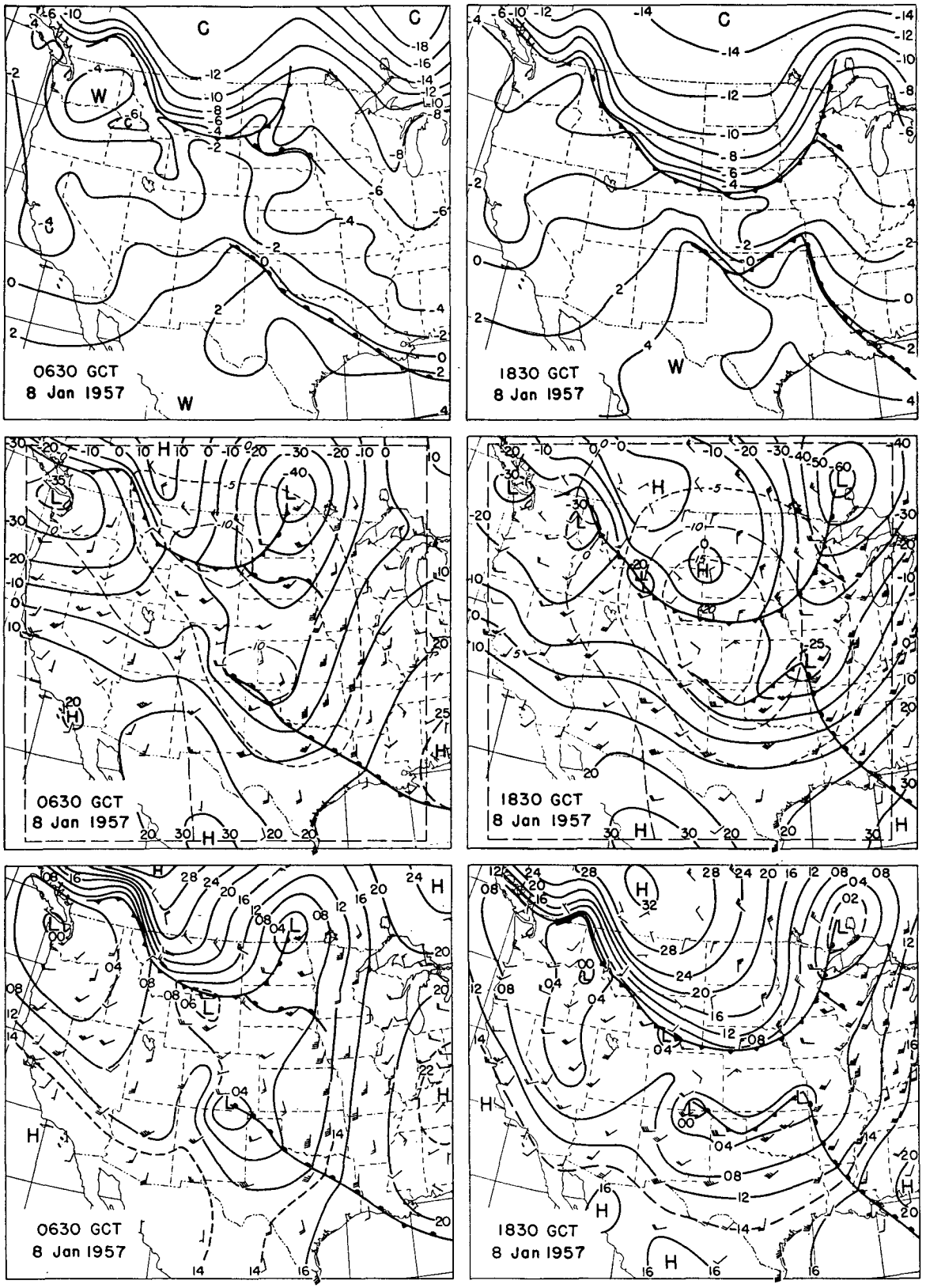

FIG. 4. Upper charts: Fronts and isopleths of the specific virtual-temperature anomaly at the earth's surface. The anomaly is expressed in per cent, a difference of one per cent corresponding roughly to an interval of 5F. Center charts: Geostrophic stream function (solid lines) and geostrophic potential function (dashed lines) for the coordinate surface $P = 10$. Unit of height is 10 gp ft. Lower charts: Sea-level isobars. Winds (in knots) are for the standard reporting level closest to 2000 ft above the coordinate surface $P = 10$, interpolated from observations at 0300, 0900, 1500, and 2100 GCT.

Fig. 4.—*Continued.*

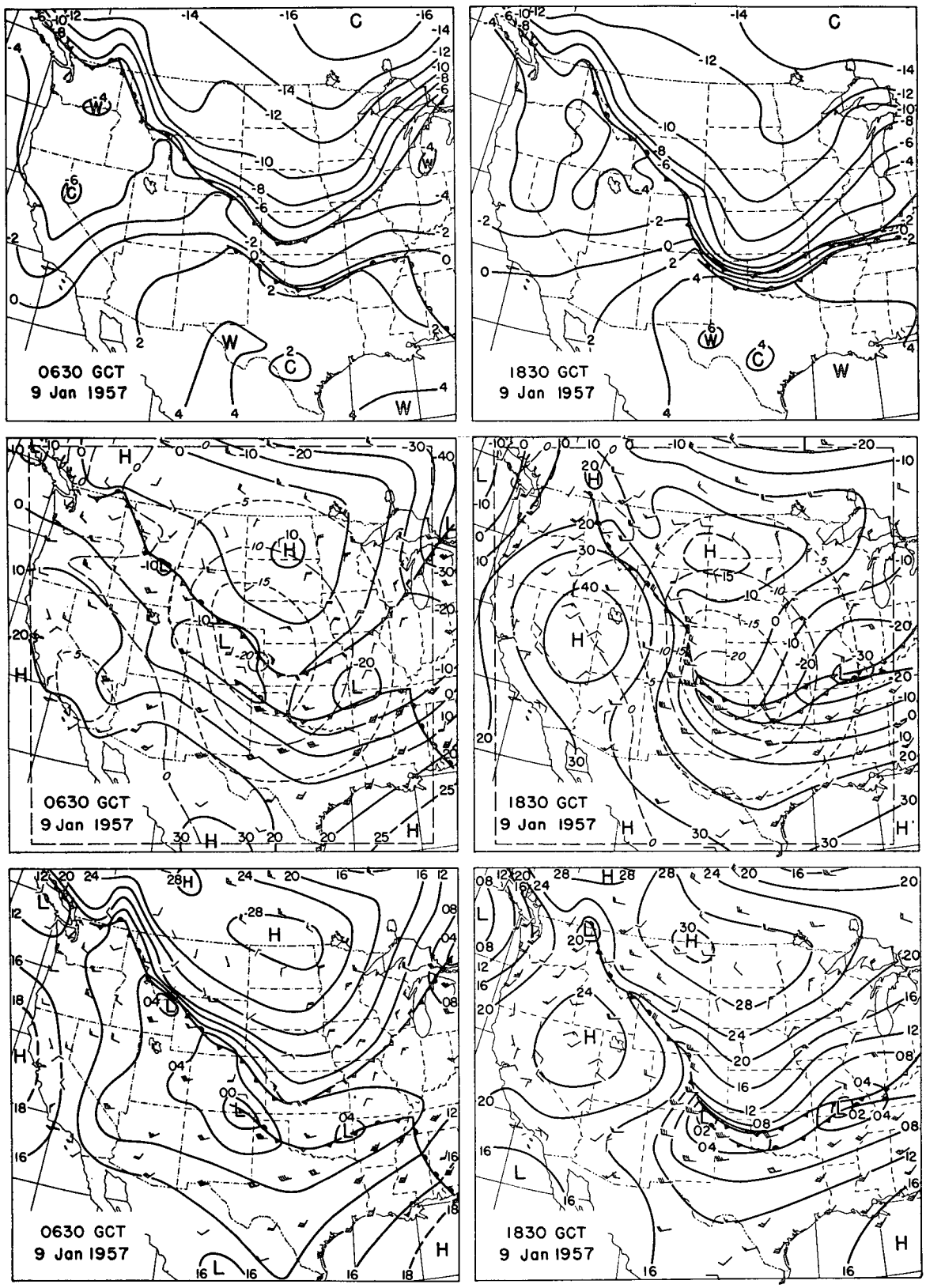

tion computations probably give too large a value for the horizontal pressure force.

By 0630 GCT 9 January, the D-values and temperatures at Lethbridge and Kimberley were +90 ft and −19F and −80 ft and +4F, respectively. The lessening of the D-value gradient between the stations is reflected in a smaller gradient of H. Since there is still an appreciable surface-temperature difference between the two stations, the sea-level charts for this time show an isobaric concentration across the Divide, largely due to the reduction process.

Particularly noticeable is the contrast between the sea-level and H- and G-charts for 0630 GCT 9 January in the Montana-Wyoming region. The sea-level chart shows an extreme concentration of isobars, whereas the stream- and potential-function fields combine to give very little apparent geostrophic wind.

The cold front which was over the Dakotas and Montana at 0630 GCT 8 January moved rapidly southeastward in spite of the fact that the sea-level isobars were nearly parallel to the front. A comparison of the cold-frontal movement with the geostrophic-wind component normal to the front computed from the two methods of representation indicates that, in general, the departure of the actual wind from the geostrophic wind is less for the charts of H and G than for the sea-level charts.

The sea-level chart for 0630 GCT 9 January shows the low over Colorado and northeastern New Mexico to be deeper than the center near the Oklahoma-Arkansas border, while the stream-function isopleths indicate the opposite situation. By 1830 GCT 9 January, the western low had disappeared from the stream-function chart, while two centers remained on the sea-level chart. The fact that, subsequent to 1830 GCT 9 January, the cold air continued to penetrate southward in the Oklahoma-Texas region indicates that the actual wind had an appreciable northerly component in the cold air behind the front. A comparison of the geostrophic winds in the vicinity of the fronts over the Great Plains obtained from the two charts for 1830 GCT 9 January suggests that perhaps the winds are not as highly ageostrophic as the sea-level chart indicates.

Of particular interest with regard to the potential-function field is the situation at 1830 GCT 9 January. The extreme temperature gradient over the panhandles of Texas and Oklahoma resulted in values of $J(Z_p, S^*)$ corresponding to geostrophic divergences (in the P-system and neglecting the variation of f with latitude) of about -1.5×10^{-4} sec^{-1}. Geostrophic-wind speeds due to the potential function alone amount to 25 to 35 kn in parts of Colorado and New Mexico. The sea-level chart does not account for this divergent portion of the geostrophic-wind field.

6. Conclusions

From the foregoing discussion, it appears safe to conclude that much of the distortion of the geostrophic-wind field which results from reduction of pressures to sea level can be avoided by the use of geostrophic stream and potential functions. A coordinate system in which a smoothed version of the earth's topography is a coordinate surface would seem to be useful in conventional as well as in numerical forecasting. The degree of smoothing which will give optimum results will depend upon the characteristic scale of the phenomena to be represented, and it is not intended to imply that the smoothing used in this paper satisfies the optimum requirements pertaining to customary synoptic systems.

Note (added in proof): The writer's attention has just recently been called to a study by Shuman in which similar ideas concerning the problem of computing and representing the horizontal pressure force have been presented. (Shuman, F. G., 1957: *On the problem of comparing station pressures at varying elevations*. Office Note No. 7, JNWPU, Washington, D. C., 10 pp.)

Acknowledgments. The writer wishes to express his gratitude to Professor Sverre Petterssen for his guidance and encouragement during the course of this investigation and to Professor George W. Platzman for numerous helpful discussions.

The Univac I of the Operations Analysis Laboratory of the University of Chicago was used for performing many of the computations involved in the construction of the charts of the geostrophic stream and potential functions. The author is much indebted to Mr. Kevin S. Tate of the staff of the Operations Analysis Laboratory, who programmed some of the computations.

The author's grateful thanks are extended to Dr. E. Paul McClain for making available averaged terrain elevations used in the construction of the smoothed topography.

REFERENCES

Bellamy, J. C., 1945: The use of pressure altitude and altimeter corrections in meteorology. *J. Meteor.*, 2, 1–79.

Bjerknes, V., and J. W. Sandström, 1910: *Dynamic meteorology and hydrography, Part I: Hydrostatics*. Washington, D. C., Carnegie Institution, 146 pp.

Collatz, L., 1955: *Numerische Behandlung von Differentialgleichungen*, 2te Auflage. Berlin, Springer-Verlag, 526 pp.

Fujita, T., and H. A. Brown, 1957: *A revised method of pressure reduction*. Tech. Rep. No. 4, Contr. No. Cwb 8950, Dept. of Meteor., The Univ. of Chicago, 8 pp.

Harrison, L. P., 1958: *Addendum to report on the problem of reduction of pressure*. Commission for Synop. Meteor., World Meteor. Org., 42 pp.

Phillips, N. A., 1957: A coordinate system having some special advantages for numerical forecasting. *J. Meteor.*, **14**, 184–185.